3-D Linear Reconstruction of the Experimental Fresnel Data by the GMMV Inversion Method

Sun, Shilong; Kooij, Bert Jan; Yarovoy, Alexander G.

DOI
10.23919/ACESS.2018.8669152

Publication date
2019

Document Version
Final published version

Published in
2018 International Applied Computational Electromagnetics Society Symposium in China, ACES-China 2018

3-D Linear Reconstruction of the Experimental Fresnel Data by the GMMV Inversion Method

Shilong Sun*, Bert Jan Kooij†, and Alexander G. Yarovoy†

*State Key Laboratory of Complex Electromagnetic Environmental Effects on Electronics and Information System
National University of Defense Technology, Changsha, 410073, China
e-mail: shilongsun@126.com;
†Faculty Electrical Engineering, Mathematics and Computer Science, Delft University of technology, The Netherlands
e-mail: B.J.Kooij@tudelft.nl; A.Yarovoy@tudelft.nl

***Abstract*—In this paper, the generalized multiple measurement vectors (GMMV) linear inversion method is applied to the reconstruction of the 3-D Fresnel data, provided by the Institue Fresnel (Marseille, France). The results show that the GMMV-based method can obtain good resolution along the x- and y- axes, while poor resolution along the z-axis, because there were only receiving antennas distributed on the x-o-y plane, indicating that the diversity of the measurement angle is critical for the GMMV method.**

I. Introduction

Nowadays, nondestructive detection is becoming more and more important in both military applications and civilian life. A wealth of reconstruction methods have been proposed over the recent decades based on certain levels of understanding to the wave propagation. Due to the high efficiency and less requirement of computing resources, the linear focusing methods have been extensively used in real applications, such as Kirchhoff migration [1], back-projection method [2], time-reversal (TR) technique [3], [4], and so forth. The imaging resolution is guaranteed by the wide bandwidth and is bound by the diffraction limit [5]. Later on, spectrum analysis technique was considered to breakthrough the diffraction limit [6]–[9]. Linear Sampling Method (LSM) [10], [11] has been proven to be effective for impenetrable scatterers, and in some cases, also applicable for dielectric scatterers [12]. Although it is efficient, the resolving ability is limited, and the discussion in comparison to the generalized multiple measurement vectors (GMMV) method is reported in [13], [14]. It is worth mentioning that the latter is capable of retrieving the shape of the scatterers and its computational complexity is linearly proportional to the number of unknowns.

In this paper, the GMMV-based shape reconstruction method is applied to the reconstruction of the 3-D Fresnel data measured by the Institut Fresnel in the year 2008 [15]. Six frequencies from 3 GHz to 8 GHz were utilized. Good resolution was obtained along the x- and y-axes, while poor resolution was observed along the z-axis, indicating that, for the GMMV linear method, the diversity of the measurement angle along one axis is critical to maintain good resolution along the same axis.

II. The GMMV-based Linear Method

A. Problem Statement

Let us consider the 3-D electromagnetic (EM) scattering problem, the scattering equation is [16]

$$\begin{aligned}&\nabla \times \boldsymbol{\mu}^{-1}\nabla \times \boldsymbol{E}_{p,i}^{\text{sct}} - \omega^2 \epsilon_{b,i}\boldsymbol{E}_{p,i}^{\text{sct}} = \omega^2 \boldsymbol{J}_{p,i},\\ &i = 1, 2, \ldots, I,\end{aligned} \tag{1}$$

where, $\boldsymbol{E}_{p,i}^{\text{inc}}$, $\boldsymbol{E}_{p,i}^{\text{sct}}$ and $\boldsymbol{E}_{p,i}^{\text{tot}}$ respectively represent the incident electric field, the scattered electric field and the total electric field of the p-th source at the i-th frequency; $\epsilon_{b,i}$ is the complex permittivity without the targets; $\boldsymbol{J}_{p,i} = \boldsymbol{\chi}_i \boldsymbol{E}_{p,i}^{\text{tot}}$ is the p-th contrast sources at the i-th frequency. Here, $\boldsymbol{\chi}_i$ is the contrast with respect to the i-th frequency.

B. The GMMV-based Linear Method

In the GMMV-based linear inversion method, the scattering domain is discretized within the FDFD scheme. The scattering operator is implemented by inverting a stiffness matrix, and the signal model can be formulated as follows

$$\boldsymbol{Y} = \boldsymbol{\Phi} \cdot \boldsymbol{J} + \boldsymbol{U} \tag{2}$$

where

$$\boldsymbol{Y} = \begin{bmatrix}\boldsymbol{y}_{1,1} & \boldsymbol{y}_{2,1} & \ldots & \boldsymbol{y}_{P,1} & \boldsymbol{y}_{1,2} & \ldots & \boldsymbol{y}_{P,I}\end{bmatrix}, \tag{3}$$

$$\boldsymbol{J} = \begin{bmatrix}\boldsymbol{j}_{1,1}^{ic} & \boldsymbol{j}_{2,1}^{ic} & \ldots & \boldsymbol{j}_{P,1}^{ic} & \boldsymbol{j}_{1,2}^{ic} & \ldots & \boldsymbol{j}_{P,I}^{ic}\end{bmatrix}, \tag{4}$$

and the operator $\boldsymbol{\Phi}[\cdot]$ is defined by

$$\boldsymbol{\Phi} \cdot \boldsymbol{J} = \begin{bmatrix}\boldsymbol{\Phi}_{1,1}\boldsymbol{j}_{1,1}^{ic} & \boldsymbol{\Phi}_{2,1}\boldsymbol{j}_{2,1}^{ic} & \ldots & \boldsymbol{\Phi}_{P,I}\boldsymbol{j}_{P,I}^{ic}\end{bmatrix}. \tag{5}$$

Here, $\boldsymbol{Y} \in \mathbb{C}^{Q \times PI}$ is the measurement data matrix, and the columns of $\boldsymbol{J} \in \mathbb{C}^{N \times PI}$ are the multiple vectors to be solved; Q represents the number of measurements, and N is the number of unknowns; $\boldsymbol{j}_{p,i}^{ic} = \omega_i \boldsymbol{j}_{p,i}$ is the normalized contrast source proportional to the induced current $\mathrm{i}\omega_i\mu_0\boldsymbol{j}_{p,i}$. $\boldsymbol{U} \in \mathbb{C}^{Q \times PI}$ represents the complex additive noises. The sum-of-ℓ_1-norm formulation and the method of solving this model were discussed in [14] in details.

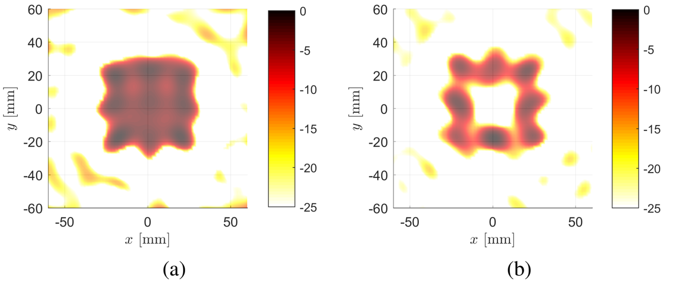

Fig. 1. The reconstructed images of the *CubeSpheres* object at 6 frequencies: $3, 4, \cdots, 8$ GHz: (a) PP-image and (b) TP-image.

III. Reconstruction results

In this section, we apply the GMMV-based shape reconstruction method to the experimental database provided by the Remote Sensing and Microwave Experiments Team at the Institut Fresnel, France, in the year 2008 [15]. In the experiments, the receiver stays in the azimuthal plane (xoy) and is rotated along two-thirds of a circle from 50° to 310° with a 10° step. The source antenna were located all round the target. The azimuthal angle θ_s ranged from 20° to 340° with a 40° step (i.e., 9 meridians) and the polar angle ϕ_s ranged from 30° to 150° with a 15° step (i.e., there were 9 parallels). The distance from the transmitter or receiver to the centre of the target has been increased to 1.796 m. Two polarization cases are measured (figure 3):

- source polarized along E_ϕ and receiver polarized along E_ϕ, corresponding to the PP data,
- source polarized along E_θ and receiver polarized along E_ϕ, corresponding to the TP data.

We refer to [15] for more description of the targets and the measurement configuration.

Let us discretize the 3-D inversion domain with 2.0 × 2.0 × 2.0 mm^3 grids. As stated in [14], the figures are shown with dB scaling, defined as follows

$$\gamma_{\text{dB}} = 10 \times \log_{10}\left(\frac{\gamma}{\max\{\gamma\}}\right). \quad (6)$$

In this paper, we have only considered the *CubeSpheres* target consisting of an aggregate of dielectric spheres. Each sphere has a diameter of 15.9 mm and a permittivity of 2.6. They were assembled so as to obtain a cube measuring 47.6 mm on each side. Fig. 1(a) and (b) give the reconstructed images by processing the PP- and TP-polarized data respectively with 6 frequencies at $3, 4, \cdots, 8$ GHz. As can be seen from the results, the basic profiles of the cube spheres can be well recovered in the PP-image, while only the basic profile is reconstructed in the TP-image. Obviously, the PP- and TP-images show different features of the objects.

Although the results of the other four targets are not shown, here we can summarize all the results of the five objects and conclude that the PP-images tend to give the details of the interior of the objects, while the TP-images tend to show the outer profile. We also remark that all the reconstructed results did not give a reasonable resolution along the z-axis, because there are no receivers distributed along z-axis. This is different with the quantitative imaging for which the incident fields must be considered, and the resolution along the z-axis is not limited by this factor.

IV. Conclusion

In this paper, the GMMV-based linearized shape reconstruction method [14] is applied to invert the 3-D Fresnel data. Multiple frequencies are jointly utilized and results show that good resolution can be obtained along the x- and y-axis. Since there are no receivers along the z-axis, we lose resolution in this direction. The diversity of the measurement angle is critical for the GMMV method, while for quantitative imaging, the incident fields are considered and the resolution is not limited to some extent by the aperture of the receiver arrays.

References

[1] W. A. Schneider, "Integral formulation for migration in two and three dimensions," *Geophysics*, vol. 43, no. 1, pp. 49–76, 1978.

[2] D. C. Munson, J. D. O'Brien, and W. K. Jenkins, "A tomographic formulation of spotlight-mode synthetic aperture radar," *Proceedings of the IEEE*, vol. 71, no. 8, pp. 917–925, 1983.

[3] M. E. Yavuz and F. L. Teixeira, "Frequency dispersion compensation in time reversal techniques for UWB electromagnetic waves," *IEEE Geoscience and Remote sensing letters*, vol. 2, no. 2, pp. 233–237, 2005.

[4] A. E. Fouda and F. L. Teixeira, "Statistical stability of ultrawideband time-reversal imaging in random media," *IEEE Transactions on Geoscience and Remote Sensing*, vol. 52, no. 2, pp. 870–879, 2014.

[5] P. Zhang, X. Zhang, and G. Fang, "Comparison of the imaging resolutions of time reversal and back-projection algorithms in EM inverse scattering," *IEEE Geoscience and Remote Sensing Letters*, vol. 10, no. 2, pp. 357–361, 2013.

[6] A. Devaney, "Time reversal imaging of obscured targets from multistatic data," *IEEE Transactions on Antennas and Propagation*, vol. 53, no. 5, pp. 1600–1610, 2005.

[7] E. A. Marengo and F. K. Gruber, "Subspace-based localization and inverse scattering of multiply scattering point targets," *EURASIP Journal on Advances in Signal Processing*, vol. 2007, no. 1, pp. 1–16, 2006.

[8] E. A. Marengo, F. K. Gruber, and F. Simonetti, "Time-reversal MUSIC imaging of extended targets," *IEEE Transactions on image processing*, vol. 16, no. 8, pp. 1967–1984, 2007.

[9] D. Ciuonzo, G. Romano, and R. Solimene, "Performance analysis of time-reversal MUSIC," *IEEE Transactions on Signal Processing*, vol. 63, no. 10, pp. 2650–2662, 2015.

[10] D. Colton and A. Kirsch, "A simple method for solving inverse scattering problems in the resonance region," *Inverse problems*, vol. 12, no. 4, p. 383, 1996.

[11] D. Colton, M. Piana, and R. Potthast, "A simple method using Morozov's discrepancy principle for solving inverse scattering problems," *Inverse Problems*, vol. 13, no. 6, p. 1477, 1997.

[12] T. Arens, "Why linear sampling works," *Inverse Problems*, vol. 20, no. 1, p. 163, 2003.

[13] S. Sun, B. J. Kooij, and A. G. Yarovoy, "A linear model for microwave imaging of highly conductive scatterers," *IEEE Transactions on Microwave Theory and Techniques*, vol. 66, no. 3, pp. 1149–1164, 2018.

[14] S. Sun, B. J. Kooij, A. G. Yarovoy, and T. Jin, "A linear method for shape reconstruction based on the generalized multiple measurement vectors model," *IEEE Transactions on Antennas and Propagation*, vol. 66, no. 4, pp. 2016–2025, 2018.

[15] J. M. Geffrin and P. Sabouroux, "Continuing with the fresnel database: experimental setup and improvements in 3d scattering measurements," *Inverse Problems*, vol. 25, no. 2, p. 024001, 2009.

[16] S. Sun, B. J. Kooij, T. Jin, and A. G. Yarovoy, "Cross-correlated contrast source inversion," *IEEE Transactions on Antennas and Propagation*, vol. 65, pp. 2592–2603, May 2017.